

Giant irreversible positive to large reversible negative magnetic entropy change evolution in Tb-based bulk metallic glass

Qiang Luo,^{1,*} Björn Schwarz,¹ Norbert Mattern,¹ and Jürgen Eckert^{1,2}

¹*Institute of Complex Materials, IFW Dresden, Helmholtzstr. 20, D-01069 Dresden, Germany*

²*Institute of Materials Science, TU Dresden, D-01062 Dresden, Germany*

(Received 18 May 2010; revised manuscript received 12 July 2010; published 27 July 2010)

We study the effects of amorphous structure and random anisotropy on the magnetic entropy change in a series of Tb-based amorphous alloys. The amorphous structure broadens the peak of magnetic entropy change and facilitates the adjustment of properties. The peak magnetic entropy change above the spin freezing temperature first depends on the average magnetic moment approximately linearly and second on the exchange interaction and random anisotropy. Large and broad reversible negative magnetic entropy changes are observed above the spin freezing temperature and giant positive irreversible magnetic entropy changes which associate with the internal entropy production are obtained well below.

DOI: [10.1103/PhysRevB.82.024204](https://doi.org/10.1103/PhysRevB.82.024204)

PACS number(s): 75.50.Kj, 61.43.Dq, 75.30.Gw, 81.05.Kf

The thermodynamic entropy illustrates that a natural process goes in the direction causing the entropy of system plus the environment to increase for an irreversible process and to remain constant for a reversible process. In a magnetic solid, the change in magnetic entropy under a field variation may result in an inverse change in the lattice and electronic entropy changes in a reversible adiabatic process, which is linked to magnetocaloric effect (MCE).¹⁻³ Extensive work has been performed on the magnetic structure and magnetic entropy change in heavy rare-earth (RE) elements and their compounds,^{2,4,5} and many other normal giant-MCE crystalline compounds,⁶⁻⁸ in which simultaneous first-order structural and magnetic phase transitions induced by temperature and/or field and/or pressure occur. Furthermore, in certain complex magnetic systems applying a magnetic field isothermally may increase the configurational entropy of spin structure. And a following adiabatic demagnetization results in heating, by a reversible increase in the lattice entropy (via the creation of phonons), which is called “inverse MCE”⁹ and has been observed mainly in two kinds of materials. In the first type, such as Fe-Rh, Mn-Ga-C, Mn-Si, and Mn-Cr(V)-Sb compounds,^{1,10-12} magnetically inhomogeneous and/or frustrated states (often one of them is antiferromagnetic) usually exist near the transition temperature, which leads to an increase in the spin disorder upon applying a field. The second kind is the Heusler-type alloys⁹ in which the positive magnetic entropy changes are mainly due to a large change in the exchange interaction as a result of the martensitic phase transformation.

Note that an irreversible process results in positive entropy production as well, which is a fascinating issue in closed and steady-state open physical chemical systems. In the case of a magnetic system with field variation only the reversible part of magnetic entropy change relates to the MCE and thus is useful for application no matter it is positive or negative. On the other side, although magnetic irreversibility relating to the dissipation energy and internal entropy production exists in all real processes, irreversible processes, and their effect on the magnetic entropy change have not been given enough attention and are poorly understood in magnetic materials. That is because first the irrevers-

ible process of magnetization itself is a challenging problem to describe since it is constantly far from equilibrium and the linear irreversible thermodynamics cannot be applied. Furthermore usually sizeable hysteretic losses and large MCE coexist in the same temperature range especially for the giant-MCE compounds with magnetostructural transformations, which makes the problem more complex due to the structure transformation and the mixed (M) phases. More commonly, the irreversible processes are artificially ignored for simplicity or are assumed to play no role arbitrarily.¹⁻⁸

Recently the MCE performances of amorphous and nanostructured materials are attracting increasing attention, owing to their some special advantages over crystalline materials.¹³⁻¹⁵ Particularly in the RE-based bulk metallic glasses (REBMGs), a large MCE has been obtained over a relatively wider temperature range compared with many giant-MCE crystalline materials.¹⁵⁻¹⁸ However, the atomic-level structure of BMGs remains much elusive and the magnetic structures in REBMGs are complicated because of the competition between random single-ion anisotropy and exchange interaction.¹⁹⁻²¹ Accordingly, the magnetic entropy change in glassy materials and its relationship with atomic and magnetic structures are not so well understood as those of crystalline materials. Concerning about the effects of reversible and irreversible magnetic processes, and amorphous structure on magnetic entropy change in amorphous materials, we investigated the magnetic properties and the magnetic entropy change in a series of Tb-based BMGs. It is found that the peak magnetic entropy change above the spin freezing temperature correlates well with average magnetic moment and depends on exchange interaction and random anisotropy as well. With decreasing temperature, the magnetic entropy change shows a reversible-and-negative to irreversible-and-positive transition, which can be understood by the interplay between exchange interaction and random magnetic anisotropy (RMA). We suggest that a determination of the irreversible process that leads to the entropy production allows evaluating the inefficiency of irreversible processes in magnetic system.

Figure 1(a) shows the temperature dependence of zero-field-cooled (ZFC) and FC magnetizations for all the

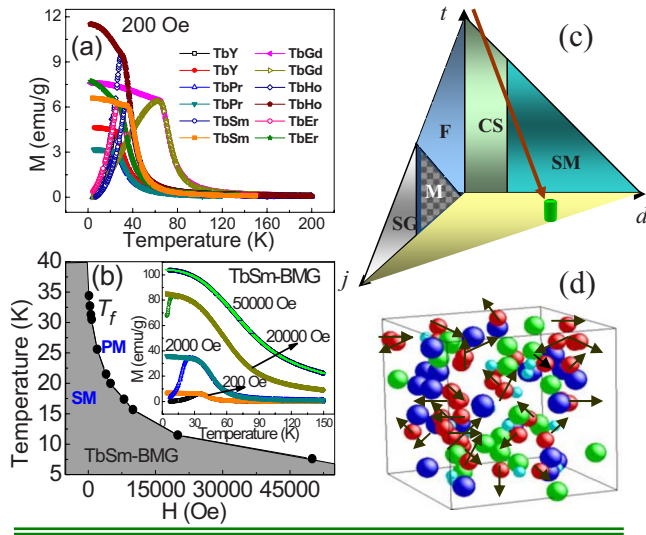


FIG. 1. (Color online) (a) Temperature dependence of the ZFC (open plots) and FC (filled plots) magnetization under 200 Oe. (b) $H(T_f)$ diagram for TbSm-BMG and the inset shows typical M_{ZFC} and M_{FC} at different fields. (c) Schematic phase diagram of magnetic states with the presence of RMA and exchange interactions. In the $d=0$ plane F, SG, and mixed (M) phases can be obtained. In the $j=0$ plane, SM and CS glass phases can be obtained. (d) Scheme of the magnetic structure for bulk amorphous alloys, the arrows indicate the directions of magnetic moments.

samples. Each ZFC curve exhibits a cusp at the spin freezing temperature, T_f [decreases with increasing field, as shown in Fig. 1(b)], near where bifurcation appears between the FC and ZFC branches indicating the beginning of irreversible process. For $4f$ RE series, single-ion anisotropy resulting from crystal (or electrostatic) fields is generally most important and depends on the specific J state of RE ion. Therefore, the magnetization and T_f vary with the alloying elements (24 K for $\text{Tb}_{36}\text{Y}_{20}\text{Al}_{24}\text{Co}_{20}$ and 64.4 K for $\text{Tb}_{36}\text{Gd}_{20}\text{Al}_{24}\text{Co}_{20}$) as a result of the change in RMA and exchange interactions (especially between Tb-RE and RE-RE). A typical schematic of the magnetic states in the presence of RMA and exchange interactions is illustrated in Fig. 1(c) ($t \equiv k_B T/J_0$, $d \equiv D/J_0$, $j \equiv \langle \Delta J \rangle/J_0$, where J_0 , D , and ΔJ are the average magnetic exchange, average strength of RMA, and exchange fluctuation, respectively). The speromagnetic (SM) phase in the $j=0$ plane relates to a frozen, random structure with strong RMA, which is obtained for our alloys below the T_f - H line in Fig. 1(b). Although having similar spin structure and dynamics with spin glasses (SGs), their origins are much different. For SG the frustration of the exchange interactions dominates, instead of RMA in SM. One should bear in mind that practical materials usually do not lie in the $d=0$ or $j=0$ plane. The line in Fig. 1(c) indicates the evolution of state for a Tb-based BMG when the temperature goes from a value far above T_f to 0 K in zero field [the final atomic and magnetic structures are sketched in Fig. 1(d)].

Typical isothermal M - H curves are displayed in Fig. 2 for $\text{Tb}_{36}\text{Sm}_{20}\text{Al}_{24}\text{Co}_{20}$. All the curves were measured with slow enough sweep rate after cooling the sample from a temperature far above T_f . It is found that the isotherm steadily drops with decreasing temperature for $T < 20$ K while increases

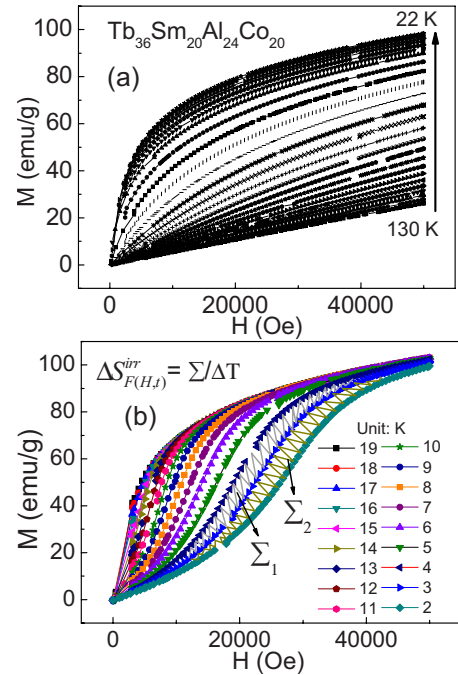


FIG. 2. (Color online) Isothermal magnetization of TbSm-BMG (a) above and (b) below 20 K.

between 20–130 K. Below 13 K S-shaped $M(H)$ curves with an inflection point at a nonzero field H_I are observed, which is related to the competition between RMA and magnetic field. The sigmoid magnetization looks similar to the field induced metamagnetic or structural transition behavior observed in the Gd-Si-Ge and Mn-Fe-P-As alloys,^{1,3,4} but with totally different origin (S-shaped curves here are observed well below T_f with smoother variation and H_I increases with decreasing temperature). In the high-field range all the low-temperature curves tend to approach the same asymptotic line resulting in a “leaf” shape of the isotherms. Similar behaviors have been observed in other alloys, indicating that addition of other RE elements does not change the strong RMA character of Tb. Magnetization processes with increasing and decreasing fields are shown in Fig. 3(a) for $\text{Tb}_{36}\text{Er}_{20}\text{Al}_{24}\text{Co}_{20}$. At 5 K there is a significant hysteresis due to the strong RMA. There is also a large hysteresis in some giant-MCE materials such as Gd-Si-Ge and Mn-Fe-P-As,^{1,3,4} which relates closely with magnetic coupled and/or field-induced first-order structural transformation. While in Gd-based BMGs with similar amorphous structure and exchange interaction (but negligible RMA), there is little hysteresis.¹⁵ With increasing temperature the hysteresis becomes smaller and smaller, and at about 15 K ($T_f \sim 27$ K for $\text{Tb}_{36}\text{Er}_{20}\text{Al}_{24}\text{Co}_{20}$) the two $M(H)$ curves nearly superpose together with little hysteresis, which is due to the rapid decrease in RMA with temperature. As pointed out by Chudnovsky,²¹ a zero-temperature SM state can convert into a correlated spin (CS) glass state above certain temperature below T_f . We suggest that the rapid change in hysteresis may relate to the gradual evolution from SM regime to CS regime. Figure 3(b) shows the evolution of M_{ZFC} with time at different temperatures below T_f for $\text{Tb}_{36}\text{Y}_{20}\text{Al}_{24}\text{Co}_{20}$. All the magnetizations increase with time indicating a glassy behav-

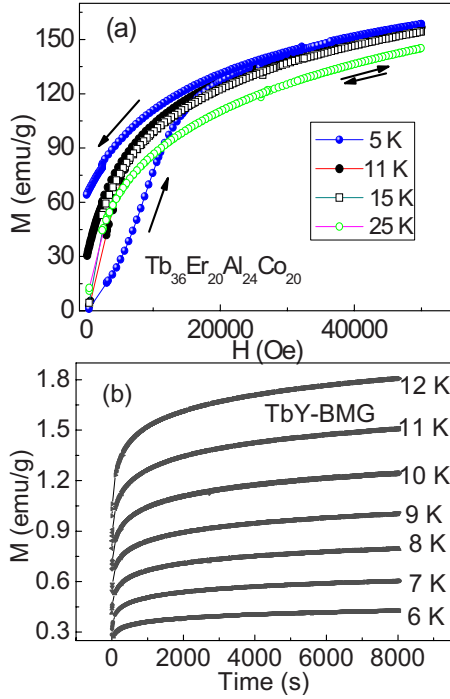


FIG. 3. (Color online) (a) $M(H)$ curves with increasing and decreasing fields and (b) evolution of M_{ZFC} with time at different temperatures.

ior. Note that the magnetization curve at lower temperatures lies below those at higher temperatures, which is in accord with the temperature and field dependences of M_{ZFC} . The spacing between two adjacent curves just slightly increases with time, suggesting that $\frac{\partial M}{\partial t}$ depends slightly on time below T_f .

The magnetic entropy change, ΔS_m , of the system can be derived from Maxwell relations: $\Delta S_m = \int_{H_{\min}}^{H_{\max}} \left(\frac{\partial M}{\partial T} \right) dH$, where H_{\min} and H_{\max} represent the initial and final values of magnetic field. Near and above the ordering temperature the above equation can be well used for our alloys due to the reversible nature. Figure 4(a) shows the $-\Delta S_m$ under a field variation of 5 T for $Tb_{36}Y_{20}Al_{24}Co_{20}$, $Tb_{36}Pr_{20}Al_{24}Co_{20}$, and $Tb_{36}Sm_{20}Al_{24}Co_{20}$. It can be seen that these alloys show very similar temperature dependence of the magnetic entropy change with a broad peak above T_f , which is of great interest to be utilized in an Ericsson cycle and associates with the amorphous structure induced fluctuation of the exchange interaction and RMA. Alloying with Ho, Er, and Gd improves the magnetic entropy change obviously compared with those BMGs alloying with Y, Pr, and Sm [see Fig. 1(a)]. Above T_f large peak values of $-\Delta S_m$: $8.94 \text{ J kg}^{-1} \text{ K}^{-1}$, $7.98 \text{ J kg}^{-1} \text{ K}^{-1}$, and $8.4 \text{ J kg}^{-1} \text{ K}^{-1}$ are obtained for $Tb_{36}Ho_{20}Al_{24}Co_{20}$, $Tb_{36}Er_{20}Al_{24}Co_{20}$, and $Tb_{36}Gd_{20}Al_{24}Co_{20}$, respectively. These values of peak magnetic entropy change, $-\Delta S_m^{PK}$, are comparable with those of Gd-based BMGs,¹⁵ pure Gd, and other RE compounds.^{2,22} The relationships between $-\Delta S_m^{PK}$ and the effective moment μ_{eff} and maximum of M_{ZFC} are shown in Figs. 4(b) and 4(c). The μ_{eff} is determined upon assuming that only the moments of RE contribute to the magnetic behavior. Because the TbY-BMG has lower concentration of magnetic atoms, we recalculate μ_{eff}

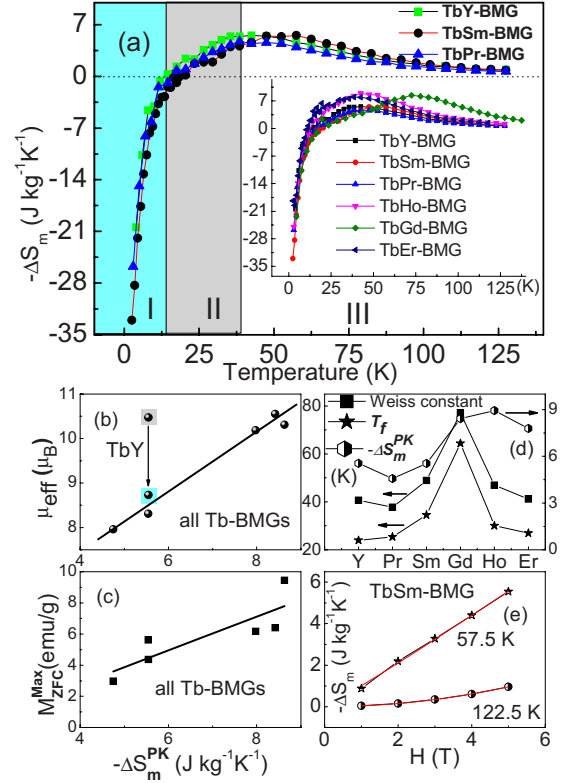


FIG. 4. (Color online) (a) Magnetic entropy changes in TbY-BMG, TbPr-BMG, and TbSm-BMG under field variation of 5 T; the inset for all alloys. (b) $-\Delta S_m^{PK}$ vs μ_{eff} and (c) M_{ZFC}^{\max} above T_f for the BMGs, the balls marked with gray and cyan squares represent the μ_{eff} values before and after considering the concentration effect for TbY-BMG. (d) Alloying dependence of the Curie constant, T_f and $-\Delta S_m^{PK}$. (e) Field dependence of magnetic entropy change at 57.5 and 122.5 K for TbSm-BMG.

alloy (to include the concentration effect of magnetic atoms) simply by supposing the both Tb and Y contribute to the moments. The roughly linear relations in Figs. 4(b) and 4(c) indicate that the peak magnetic entropy change is correlated well with magnetic moment in amorphous materials. The alloying RE-dependent behaviors in Fig. 4(d) indicate that the Curie constant and T_f show a peak at Gd and then decrease rapidly while $-\Delta S_m^{PK}$ shows a peak at Ho and then reduces slightly. There difference suggests that $-\Delta S_m^{PK}$ depends more on magnetic moment than exchange coupling. Figure 4(e) shows the field dependence of $-\Delta S_m$ at 57.5 K ($-\Delta S_m^{PK}$) and 122.5 K, which can be fitted (red lines) using $|\Delta S_m| \propto H^n$ (in a mean-field case) with $n=1.06$ at 57.5 K and 1.99 at 122.5 K. Far above T_f , $n \approx 2$ is a consequence of the Curie-Weiss law, and n decreases with decreasing temperature as the Curie-Weiss law deviates and the short-range magnetic order forms gradually. The n values at $T_p \sim 57.5 \text{ K}$ ($n=1.06$) and $T_f \sim 34.5 \text{ K}$ ($n=0.89$) are larger than $2/3$ predicted by the mean-field model and those of Fe-based glassy ribbons ($n \sim 0.73$).¹⁴ The increase in n may arise from the impact of RMA on the cluster formation and magnetic behavior.

At temperatures well below T_f interpretation of the results from application of Maxwell relation should be done with

caution due to the irreversible process. Borrowing the method adopted in the reversible region, we calculated the area between magnetic isotherms at neighboring temperatures, and then got the entropy change after dividing by the temperature difference [Fig. 2(b)]. We call it, $\Delta S_{F(H,t)}^{irr}$, which has a different meaning than ΔS_m (or ΔS_m^{rev}) obtained in the high-temperature range, because $\Delta S_{F(H,t)}^{irr}$ is almost irreversible and depends on sample's thermal history, $F(H,t)$. The weak dependence of $\frac{\partial M}{\partial T}$ on time [Fig. 3(b)] suggests that $\Delta S_{F(H,t)}^{irr}$ also depends weakly on time. Since the positive $\Delta S_{F(H,t)}^{irr}$ is history dependent, it provides valuable information (about the RMA, local magnetic structures, the internal entropy production) when the following conditions are satisfied: (a) the initial state and magnetization process are well defined; (b) the system is homogenous and its relaxation time is well separated from the experimental time scale so that the system can be considered to comprise small subsystems (infinitesimal droplets); (c) $\Delta S_{F(H,t)}^{irr}$ can be well determined and understood when it almost has nothing to do with the reversible process. By this method, all the alloys exhibit giant positive magnetic entropy changes in the lowest temperatures as shown in Fig. 4(a). At 2.5 K the $\Delta S_{F(H,t)}^{irr}$ at a filed variation of 5 T corresponds to about $33 \text{ J kg}^{-1} \text{ K}^{-1}$ for $\text{Tb}_{36}\text{Sm}_{20}\text{Al}_{24}\text{Co}_{20}$. As illustrated in Fig. 4(a), the temperature dependence of magnetic entropy change can be divided into three parts obviously. In the exchange dominating region III, the exchange interaction is becoming stronger compared with the thermal energy with decreasing temperature, which results in an increase in magnetization and magnetic entropy change. And the RMA increases slowly and begins to influence the spin structure and slows down the spin flipping with decreasing temperature. In the competitive region II, the RMA increases gradually to a value comparable with the exchange interaction and the magnetic entropy change decreases gradually on decreasing temperature. In the RMA dominating region I, the RMA increases rapidly with decreasing temperature, which results in a giant positive $\Delta S_{F(H,t)}^{irr}$. Further, $\Delta S_{F(H,t)}^{irr}$ increases with increasing field as shown in Fig. 5(a) for $\text{Tb}_{36}\text{Sm}_{20}\text{Al}_{24}\text{Co}_{20}$. At a field change of 1 T, $\Delta S_{F(H,t)}^{irr}$ shows a shallow minimum below 20 K; with increasing field the peak narrows and moves to lower temperature (at 4 and 5 T there is no peak observed), which suggests the interplay of RMA and external field.

In crystalline materials the anisotropy aligns moments along preferred directions determined by the long-range crystalline order, which results in a dependence of the magnetic properties on the crystallographic direction.¹ Further both experimentally and theoretically it was pointed out to use anisotropic materials to increase the refrigerant capacity.^{23–26} Note that for crystalline materials with strong magnetocrystalline anisotropy, the system may possess soft magnetic behavior due to the weak impediments (from structural disorder or defects) to domain-wall movements. However, due to the wholly disordered structure, the magnetic properties are macroscopically isotropic in BMGs. In REBMGs the RMA breaks the long-range ferromagnetic (F) order and orients strongly the spin along their local anisotropy axes, which brings about complex ground states and irreversibility.^{19–21} It is the competition between exchange

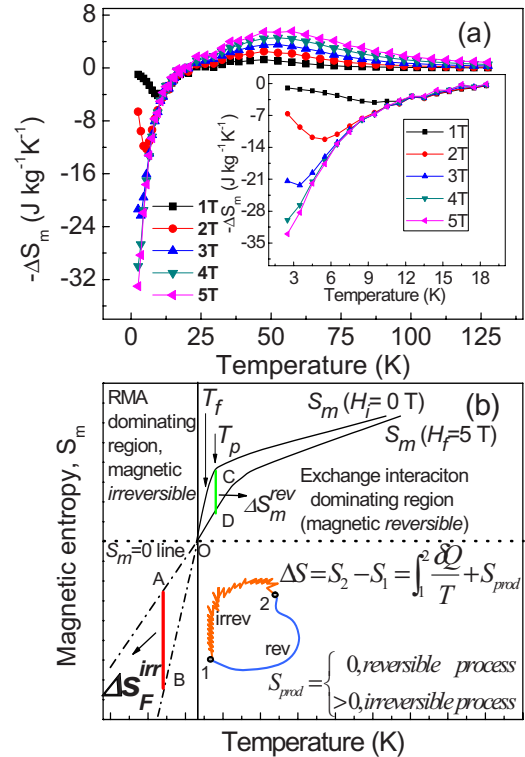


FIG. 5. (Color online) (a) Magnetic entropy changes for TbSm-BMG at different fields. (b) A sketch map illustrating the temperature-dependent magnetic entropy at two fixed external fields in RMA system. The dashed-dotted lines (O-A and O-B below $S_m = 0$ line) only relate to the measured states just as stated in our measurement and have nothing to do with the thermal equilibrium states due to the magnetic irreversibility, where positive irreversible magnetic entropy is obtained. It is magnetic reversible in states C and D where normal reversible negative magnetic entropy change is obtained. The down inset shows generally the entropy changes in a closed system in a reversible process and an irreversible process for a comparison.

interaction and RMA that leads to the continuous evolution of magnetic entropy change in the Tb-based BMGs, which is different from those of the exchange interaction dominating Gd-based BMGs and Fe(Co)-based glassy ribbons, and the crystalline materials with strong magnetocrystalline anisotropy.^{14,15,23} Actually the RMA influences the magnetic-cluster forming and spin dynamics from certain temperature above T_f . The relaxation time, typically on the order of seconds in strong RMA systems as T_f is approached from above, is several orders of magnitude higher than that in SG.¹⁹ The peak temperatures of $-\Delta S_m(T_p)$ are usually larger than T_f in Tb-based BMGs ($T_p \sim 1.5-2T_f$) and the maximum of $-\Delta S_m$ is smaller than those of Gd-based BMGs.¹⁵ We attribute these results partly to the already existing short-range magnetic clusters and the RMA near and above T_f , which make the maximum $-\Delta S_m$ do not locate closely near the ordering temperature and as well cause some entropy loss due to the energy required to realign the random spins constrained by RMA.

Figure 5(b) illustrates schematically the evolution of magnetic entropy for RMA systems. In an ideal reversible case,

the increase in magnetic entropy by adiabatic demagnetization leads to reduction in the lattice and electronic entropy in the same amount in normal MCE materials, resulting in cooling. Whereas in the inverse MCE materials, the reversible positive magnetic entropy change indicates that the adiabatic magnetization results in cooling. Whereas, the irreversible positive magnetic entropy here relates to the entropy production [in any irreversible process internal entropy is always produced, $S_{prod} > 0$, see Fig. 5(b)]. The positive $\Delta S_{F(H,t)}^{irr}$, as a measure of S_{prod} , indicates that substantial energy (via the annihilation of phonons and consumption of external energy) is consumed to overcome the RMA for the realign of spins under a field variation. The increase in $\Delta S_{F(H,t)}^{irr}$ with decreasing temperature suggests that more and more energy is degraded or wasted accompanied with a higher degree of irreversibility. Furthermore, we should stress the differences between the irreversibility observed here and that in some first-order magnetic phase transition giant-MCE materials.¹ In these crystalline systems, the irreversibility comes from the impediments of defects to domain-wall motion; and distinct hysteresis and giant MCE may coexist in the same temperature range (sometimes relates to the mixed phases).^{27,28} The situation for Tb-based BMGs is different since: first they display second-order magnetic phase transition, and the hysteresis is mainly due to the RMA and does not relate to structural transition; second the irreversible process dominates well below the spin freezing temperature where there is only a single phase, and the reversible and irreversible processes are well separated in both the low- and high-temperature regions. These differences permit the simplicity and coherence to describe the magnetic entropy change in Tb-based BMGs in the whole temperature range.

In conclusion, this study indicates that (1) average mag-

netic moment, and the concentration of magnetic atoms, the RMA and exchange interaction have different impacts on the magnetic entropy change in amorphous materials, which can be tuned easily by careful selection of compositions, alloying, and heat treatment. (2) From the perspective of application, the RMA brings negative impact on MCE because it leads to the irreversibility. Nevertheless, the irreversible positive magnetic entropy change, $\Delta S_{F(H,t)}^{irr}$ reflects the amount of internal energy dissipation, and provides a means for measuring the various inefficiencies encountered in practical operations (in a reversible process, the magnitude of negative magnetic entropy change can be considered as a measure of magnetic refrigerant capacity). Through the researches of ΔS_m^{rev} and $\Delta S_{F(H,t)}^{irr}$, one can obtain not only the distribution and evolution of entropy, but also the information about the magnetic anisotropy and exchange interaction, which still remain to be settled in detail. For practical application, future works should be dedicated to find some smart strategy to control short-to-medium range ordered magnetic/aromatic structures of amorphous magnets in order to obtain reversible giant magnetic entropy change in a wide temperature span. Theoretically, a comprehensive exploration of the reversible and irreversible magnetic processes, and a deeper understanding of the magnetic ordering process and the relationship between structure and entropy both in amorphous and crystalline materials are urgently needed.

The authors thank K. Zhao and W. H. Wang, Institute of Physics, Chinese Academy of Science, for providing some of the samples. G. Wang, J. Liu and Y. Zhang in IFW Dresden are acknowledged for stimulating discussions and experimental assistance. Financial support from the National Humboldt Foundation is gratefully acknowledged.

*q.luo@ifw-dresden.de

¹O. Tegus, E. Brück, L. Zhang, Dagula, K. H. J. Buschow, and F. R. de Boer, *Physica B* **319**, 174 (2002).

²V. K. Pecharsky and K. A. Gschneidner, Jr., *J. Magn. Magn. Mater.* **200**, 44 (1999).

³O. Tegus, E. Brück, K. H. J. Buschow, and F. R. de Boer, *Nature (London)* **415**, 150 (2002).

⁴W. Choe, V. K. Pecharsky, A. O. Pecharsky, K. A. Gschneidner, V. G. Young, and G. J. Miller, *Phys. Rev. Lett.* **84**, 4617 (2000).

⁵V. K. Pecharsky and K. A. Gschneidner, Jr., *Phys. Rev. Lett.* **78**, 4494 (1997).

⁶B. G. Shen, J. R. Sun, F. X. Hu, H. W. Zhang, and Z. H. Cheng, *Adv. Mater.* **21**, 4545 (2009).

⁷J. Marcos, A. Planes, L. Mañosa, F. Casanova, X. Batlle, A. Labarta, and B. Martínez, *Phys. Rev. B* **66**, 224413 (2002).

⁸S. L. Molodtsov, M. Richter, S. Danzenbächer, S. Wieling, L. Steinbeck, and C. Laubschat, *Phys. Rev. Lett.* **78**, 142 (1997).

⁹T. Krenke, E. Duman, M. Acet, E. F. Wassermann, X. Moya, L. Mañosa, and A. Planes, *Nature Mater.* **4**, 450 (2005).

¹⁰S. A. Nikitin, G. Myalikgulyev, A. M. Tishin, M. P. Annaorazov, K. A. Asatryan, and A. L. Tyurin, *Phys. Lett. A* **148**, 363 (1990).

¹¹Y. Q. Zhang and Z. D. Zhang, *J. Alloys Compd.* **365**, 35 (2004).

¹²T. Tohei, H. Wada, and T. Kanomata, *J. Appl. Phys.* **94**, 1800

(2003).

¹³M. Foldeaki, R. Chahine, B. R. Gopal, T. K. Bose, X. Y. Liu, and J. A. Barclay, *J. Appl. Phys.* **83**, 2727 (1998).

¹⁴V. Franco, C. F. Conde, J. S. Blázquez, A. Conde, P. Švec, D. Janičkovič, and L. F. Kiss, *J. Appl. Phys.* **101**, 093903 (2007).

¹⁵Q. Luo, D. Q. Zhao, M. X. Pan, and W. H. Wang, *Appl. Phys. Lett.* **89**, 081914 (2006); and **90**, 211903 (2007).

¹⁶H. Fu, X. Y. Zhang, H. J. Yu, B. H. Teng, and X. T. Zu, *Solid State Commun.* **145**, 15 (2008).

¹⁷L. Liang, X. Hui, and G. L. Chen, *Mater. Sci. Eng., B* **147**, 13 (2008).

¹⁸Q. Luo and W. H. Wang, *J. Non-Cryst. Solids* **355**, 759 (2009).

¹⁹Q. Luo, D. Q. Zhao, M. X. Pan, and W. H. Wang, *Appl. Phys. Lett.* **92**, 011923 (2008).

²⁰C. Jayaprakash and S. Kirkpatrick, *Phys. Rev. B* **21**, 4072 (1980).

²¹E. M. Chudnovsky, *J. Appl. Phys.* **64**, 5770 (1988).

²²P. J. von Ranke, V. K. Pecharsky, and K. A. Gschneidner, *Phys. Rev. B* **58**, 12110 (1998).

²³M. S. Reis, R. M. Rubinger, N. A. Sobolev, M. A. Valente, K. Yamada, K. Sato, Y. Todate, A. Bouravleuv, P. J. von Ranke, and S. Gama, *Phys. Rev. B* **77**, 104439 (2008).

²⁴A. L. Lima, K. A. Gschneidner, and V. K. Pecharsky, *J. Appl.*

- [Phys.](#) **96**, 2164 (2004).
- ²⁵R. I. Bewley and R. Cywinski, [Phys. Rev. B](#) **54**, 15251 (1996).
- ²⁶J. Chappert, L. Asch, M. Bogé, G. M. Kalvius, and B. Boucher, [J. Magn. Magn. Mater.](#) **28**, 124 (1982).
- ²⁷G. J. Liu, J. R. Sun, J. Shen, B. Gao, H. W. Zhang, F. X. Hu, and B. G. Shen, [Appl. Phys. Lett.](#) **90**, 032507 (2007).
- ²⁸J. S. Amaral and V. S. Amaral, [Appl. Phys. Lett.](#) **94**, 042506 (2009).